

# Reproducible Gating for High-Resolution Flow Cytometric Characterization of Extracellular Vesicles in Next-Generation Biomarker Studies

Ishwor Thapa<sup>1</sup><sup>a</sup>, Yohan Kim<sup>2</sup><sup>b</sup>, Fabrice Lucien<sup>2</sup><sup>c</sup> and Hesham Ali<sup>1</sup><sup>d</sup>

<sup>1</sup>College of Information Science and Technology, University of Nebraska at Omaha, Omaha, U.S.A.

<sup>2</sup>Department of Urology, Mayo Clinic, Rochester, U.S.A.

**Keywords:** Extracellular Vesicles, High Resolution Flow Cytometry, Automated Gating, Reproducibility and Robustness, Biological Signals, FCS.


**Abstract:** With the continuous advancements of biomedical technologies, we have access to instruments capable of producing new types of biological data or generating traditional data with higher degrees of quality. With the support of such data, researchers and practitioners continue to explore the possibilities of developing new approaches to obtain valuable data-driven signatures or biosignals to be used for diagnosis, classification, or assessment of treatments. However, with the emergence of new types of data, it is often the case that they are available in raw formats that are not suitable for extracting the needed biomarkers. Hence, much work is needed to process the raw data sets obtained from new medical instruments and transform the signals into products capable of capturing the desired knowledge. Next-generation biomarkers such as “liquid biopsies” are emerging tools to improve cancer diagnostics, disease stratification, and treatment monitoring. As potential cancer biomarkers, circulating Extracellular Vesicles (EV) levels may early-predict disease recurrence and resistance to treatment. High-resolution flow cytometry (hrFC) is a sensitive and high-throughput method for quantifying circulating levels of EVs with minimal sample processing. One of the benefits of using hrFC is that there is no need to isolate or purify the molecules of interest from the biological samples prior to running the flow. However, signals in hrFC data currently depend on manual and subjective approaches to gating the positive events. Such approaches are often time-consuming, error-prone, and lack the levels of robustness and reproducibility needed to trust the obtained information. This study proposes an automated quantitative technique to process flow cytometry data for EVs with a high degree of accuracy consistency. A publicly available Shiny web application is presented that performs quality check of flow cytometry files and automated gating of biosignals, viz. subpopulations of EVs that are of interest to next generation biomarker studies.


## 1 INTRODUCTION


According to the International Society for Extracellular Vesicles (ISEV), extracellular vesicle (EV) is a generic term for particles naturally released from the cell that are delimited by a lipid bilayer and cannot replicate, i.e. do not contain a functional nucleus (Théry et al., 2018). EVs are heterogenous in size ( $<100nm$  to  $>1\mu m$ ) and their distribution follows a power-law function, meaning that the large


number of EVs of small size are observed and the concentration of EVs decreases with increasing size. EVs are released by normal and malignant cells in body fluids such as blood and urine. Various studies have shown that circulating EVs may be the next-generation of biomarkers for the management of multiple diseases including cancers, neurodegenerative diseases and chronic liver diseases (Lucien et al., 2022), (Samuel et al., 2018), (Pan et al., 2023), (Ellison et al., 2023), (Ohmichi et al., 2019), (Aharon et al., 2020), (Newman et al., 2022).

EVs can be extracted from biofluids like plasma and urine in a wet-lab setting. This is of great significance in a clinical setting because with this technology, EVs can directly be characterized from

<sup>a</sup> <https://orcid.org/0000-0002-3594-1631>

<sup>b</sup> <https://orcid.org/0000-0002-2378-0068>

<sup>c</sup> <https://orcid.org/0000-0001-6149-345X>

<sup>d</sup> <https://orcid.org/0000-0002-8016-6144>

the biofluids. The isolation of EVs are often complemented with antibody labeling of known markers such as *Mammaglobin-A* in breast cancer plasma samples and *PSMA* in prostate cancer plasma or urine samples to identify cancer marker enriched EVs (Salmond et al., 2021), (Lucien et al., 2022). The diluted EV fractions are then run through High Resolution Flow Cytometry (hrFC) allowing high-throughput detection and immunophenotyping of EVs at the single-particle level (Kim et al., 2022). Using hrFC, it was observed that the levels of circulating prostate cancer-specific extracellular vesicles (PCEVs) were found to be the highest in metastatic castration-resistant prostate cancer (mCRPC) patients and were the lowest in localized prostate cancer (Lucien et al., 2022). To address variability in EV experiments, two initiatives viz. a) calibration of flow cytometers in standard units and standardization of detected EV concentration (van der Pol et al., 2018), and b) transparent reporting (Welsh et al., 2020b) have been established. The MIFlowCyt-EV framework requires standardization of reporting the steps undertaken, including experiment design, sample preparation, assay control, instrument calibration and data acquisition (Welsh et al., 2020b). The implementation of this framework is adapted into a public repository for EV flow cytometry data (Arce et al., 2023). Additionally, Welsh et al. have developed FCMPass software that provides a new method to standardize light scatter utilizing the instrument specific sensitivity parameters (Welsh et al., 2020a).

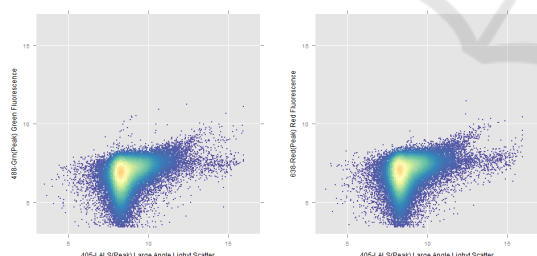


Figure 1: Representative figure to show scatter plots of two different fluorescence channels versus the large angle side scatter channel.

For each captured EV particle, the forward-scattered light, side-scattered light and dye-specific fluorescence signals are captured and represented numerically in a standard data file, called Flow Cytometry Standard (FCS) files. The FCS files can be visualized in scatter plots with different channels on X and Y axes. For example, in Figure 1, two different fluorescence channels are plotted against the large angle side scatter channel (LALS).

An objective method of quantification of EV lev-

els is critical in establishing the circulating EVs as the next-generation of biomarkers. The current challenge in analyzing the flow cytometry data of EVs is the manual gating (filtering) step where the population of EVs that are potential markers for a biological condition are separated from background noise. Manual gating is not only time-consuming and user-dependent but also error-prone, which ultimately can result in irreproducible data. Our research goal is to develop an automated quantitative technique to facilitate the manual gating process, which is key to next-generation biomarker studies. We propose two automated gating techniques, viz. a) rectangular gating and b) five-sided gating. In rectangular gating, the algorithm is straight-forward and is primarily based on minimum size of the particle and its fluorescence level. However, this approach still captures some EVs whose fluorescence doesn't increase linearly with the size. To reduce false positives, an additional point is added in the gate to filter out EVs, which are larger in size but not as fluorescent. Furthermore, we have developed a web application based on Shiny R package to allow biomedical researchers to upload a FCS file from hrFC and obtain number of positive events in a sample using automated gating. Our tool also summarizes the number of events for every second over the duration of acquisition time in Flow Cytometry. This provides a quality checking step in the processing of hrFC and is a critical feature that can identify flow runs that are prone with errors. The results of gating obtained using the proposed automated gating pipeline show that it accurately identifies the disease specific EV sub-population in an unbiased manner and produces results comparable to that of manual gating from experienced users. Additionally, the method can be extended to identify unique sub-population of EVs that can serve as significant features in machine learning-based classification.

## 2 DATASET AND METHODS

### 2.1 EV Labeling and Quantification

In our previous work, we presented a strategy for standardization of acquisition parameters for side-scatter detection of extracellular vesicles (EVs) and other particles from cell-depleted plasma and urine (Kim et al., 2022). In this process, optimal acquisition settings such as illumination wavelength power, side scatter triggering threshold, and flow rate for cytometer (Apogee A60-Micro Plus) have been derived to improve the sensitivity of EV detection. *PSMA* and *STEAP1* antibodies were labeled with two

Alexa Fluor (AF647 and AF488) antibody labeling kits. With desired concentration of urine and antibody mixture, the antibody-biofluid mixture can be incubated to label prostate specific EVs with the antibodies. Next, three technical replicates from urine samples of thirty cancer patients were run on Apogee A60-Micro Plus (A60MP, Apogee Flow Systems Inc., Northwood, UK) cytometer for 60 seconds as described in our previous work (Kim et al., 2022). For each run, the resulting data from cytometer are saved in a FCS file.

## 2.2 FCS Files

The Flow Cytometry Standard (FCS) file provides specifications and experimental data that includes the light scatter and fluorescence measurements (Spidlen et al., 2021), (Spidlen et al., 2010). The information stored in FCS files can be read in a programming language like R using packages such as flowCore (Hahne et al., 2009). The flowCore package allows creation of a *flowFrame*, a container storing all the metadata and events captured in the Flow cytometry experiments (Hahne et al., 2009). The experiment data is stored in a matrix format that can be accessed from the *exprs* slot of the *flowFrame* object. The rows of this matrix represent the events and columns represent different measurement channels including light scatter and fluorescence.

## 2.3 Quality Check Reporting

In the data section of information stored in FCS file, the *TIME* variable is also stored that depicts the time point of the event being recorded. The number of events for every second is computed and is visualized as a plot with additional mean and standard deviation values (see Figure 2). It can also show how the number of events changes over time and can be used to assess flow rate stability and artifacts (e.g. bubbles) that could occur during acquisition and influence quantitative analysis. In addition, boxplots are generated for each channel to check any aberrant pattern in scatter and fluorescence acquisition (see Figure 5).

## 2.4 Automated Gating for Enumeration of EVs

Scatter plots such as one in Figure 1 show more than 49,000 events captured, among which majority of the events belong to background noise and a small number of events (about 0.14% left and 0.33% right) are positive events. Positive events are the EVs labeled with a fluorescent antibody against a specific marker

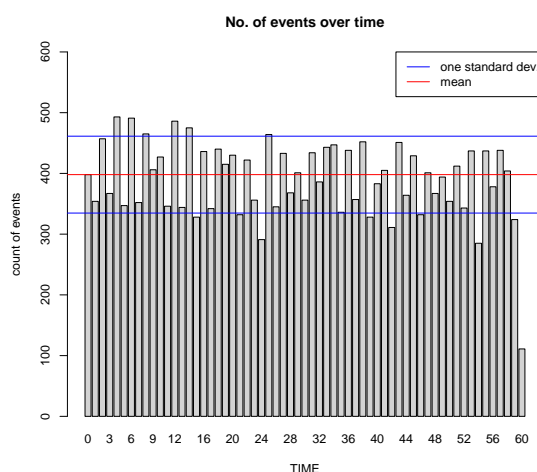


Figure 2: Total events captured per second.

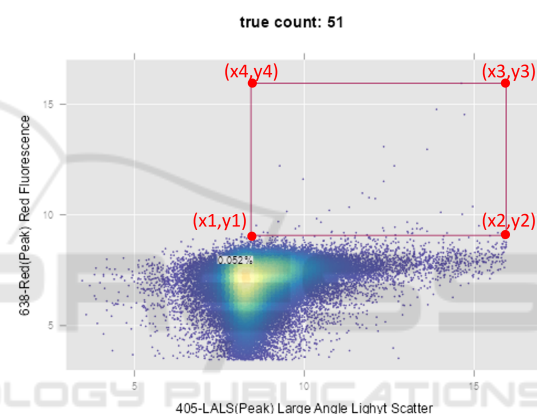


Figure 3: Rectangular gate for identification of sub-population of events.

and are characterized by linear relationship between these channel readings.

One of the major limitations in the reproducibility of EV studies is the manual gating of EVs. The gating process involves manual creation of boundaries on the scatter plot using tools such as FlowJo to count the events inside the boundaries. This manual step is error-prone and can vary for different individuals who gate these events. In order to overcome these challenges, two automated gating strategies have been developed to enumerate the positive EVs. The automated gating mechanisms involve identifying the starting position for gate and finding the rest of gating coordinates. In the first strategy, we describe a rectangular gating scheme based on minimum size of the particle and its fluorescence. Since bigger EVs will have greater surface area to accommodate binding of more number of surface markers, the dye-specific fluorescence signal is expected to be higher. Hence, we describe five-sided gating based on size exclusion cri-

teria of EVs and linear scaling of fluorescence with the size. We then compare the results of the automated gating to that of manual gating by two independent reviewers.

**Algorithm 1:** Algorithm for rectangular automatic gating of EVs. The points  $x[1-4]$  and  $y[1-4]$  refers to the points of gates as shown in Figure 3.

**Data:**  $X1$  := lower limit of the EV size,  $inputMatrix$  is matrix of measurements with ‘n’ events as rows and ‘m’ columns as channels

**Result:**  $(x1, y1, x2, y2, x3, y3, x4, y4)$

```

1 transformed := arcsinh(inputMatrix);
2 X := transformed[1 : n, 'LALS'];
3 Y := transformed[1 : n, 'RedChannel'];
4 x1 := arcsinh(X1);
5 densityY := density(Y);
6 poi := pointOfInflection(densityY);
7 y1 := abscissa(poi) +
    distance(peak(densityY), poi);
8 x2 := max(X);
9 y2 := y1;
10 x3 := max(X);
11 y3 := max(Y);
12 x4 := x1;
13 y4 := max(Y);
14 return
    (polygonGate(x1, y1, x2, y2, x3, y3, x4, y4));
    
```

#### 2.4.1 Rectangular Gating

The gating involves plotting the EV particle size on X-axis and fluorescence channel measurement on Y-axis. A side scatter triggering threshold set at 2,300 arbitrary units (a.u.) on X-axis will be set as  $x1$ . This marks the minimum size of the EVs. For identifying the first point on Y-axis ( $y1$ ), peak density of the fluorescence values is identified and point of inflection in the downward slope of the density plot after the peak is determined. The value of  $y1$  is set to the sum of abscissa of point of inflection and distance between point of inflection and peak. This ensures that the background noise region in fluorescence axis is avoided to begin the gating (see Figure 3). This is a critical step in capturing the signal. Hence, it is described independently as rectangular gating and all the steps in this approach are listed in **Algorithm 1**.

#### 2.4.2 Five-Sided Gating

The rectangular gating has few shortcomings. Among the larger EVs, those that do not exhibit elevated fluorescence may be misclassified as true positives be-

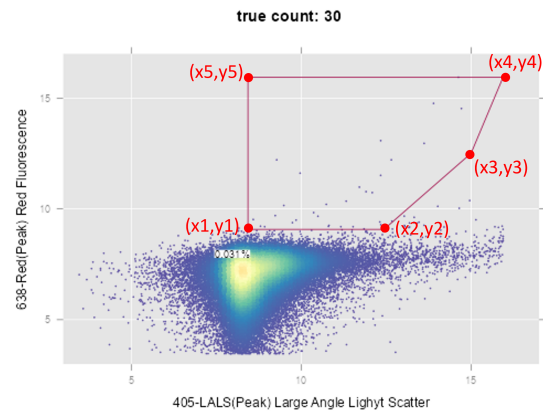


Figure 4: Five-sided gate for identification of sub-population of events.

**Algorithm 2:** Algorithm for five-sided automatic gating of EVs. The points  $x[1-5]$  and  $y[1-5]$  refers to the points of gates as shown in Figure 4.

**Data:**  $X1$  := lower limit of the EV size,  $X2$  := higher limit of the EV size,  $inputMatrix$  is matrix of measurements with ‘n’ events as rows and ‘m’ columns as channels

**Result:**  $(x1, y1, x2, y2, x3, y3, x4, y4, x5, y5)$

```

1 transformed := arcsinh(inputMatrix);
2 X := transformed[1 : n, 'LALS'];
3 Y := transformed[1 : n, 'RedChannel'];
4 x1 := arcsinh(X1);
5 densityY := density(Y);
6 poi := pointOfInflection(densityY);
7 y1 := abscissa(poi) +
    distance(peak(densityY), poi);
8 x2 := arcsinh(X2);
9 y2 := y1;
10 x4 := max(X);
11 y4 := max(Y);
12 x3 := [x4];
13 y3 := y2 + (y4 - y2)/2;
14 x5 := x1;
15 y5 := y4;
16 return
    (polygonGate(x1, y1, x2, y2, x3, y3, x4, y4, x5, y5));
    
```

cause larger EVs typically have increased fluorescence due to their size. Incorporating this information as a criteria to filter noise is critical in accurately identifying positive EVs. Based on the input from hrFC experts in the team, rectangular gating is fine-tuned to add a threshold of maximum size of EV. **Algorithm 1** is updated to limit the size of EV to a specified value (123,000 a.u.). In addition, one more polygon point is added in between the minimum and maximum fluorescence. This point ( $x3, y3$ ) as shown in Figure 4 will aid in filtering the points whose fluorescence doesn't scale linearly with EV size.

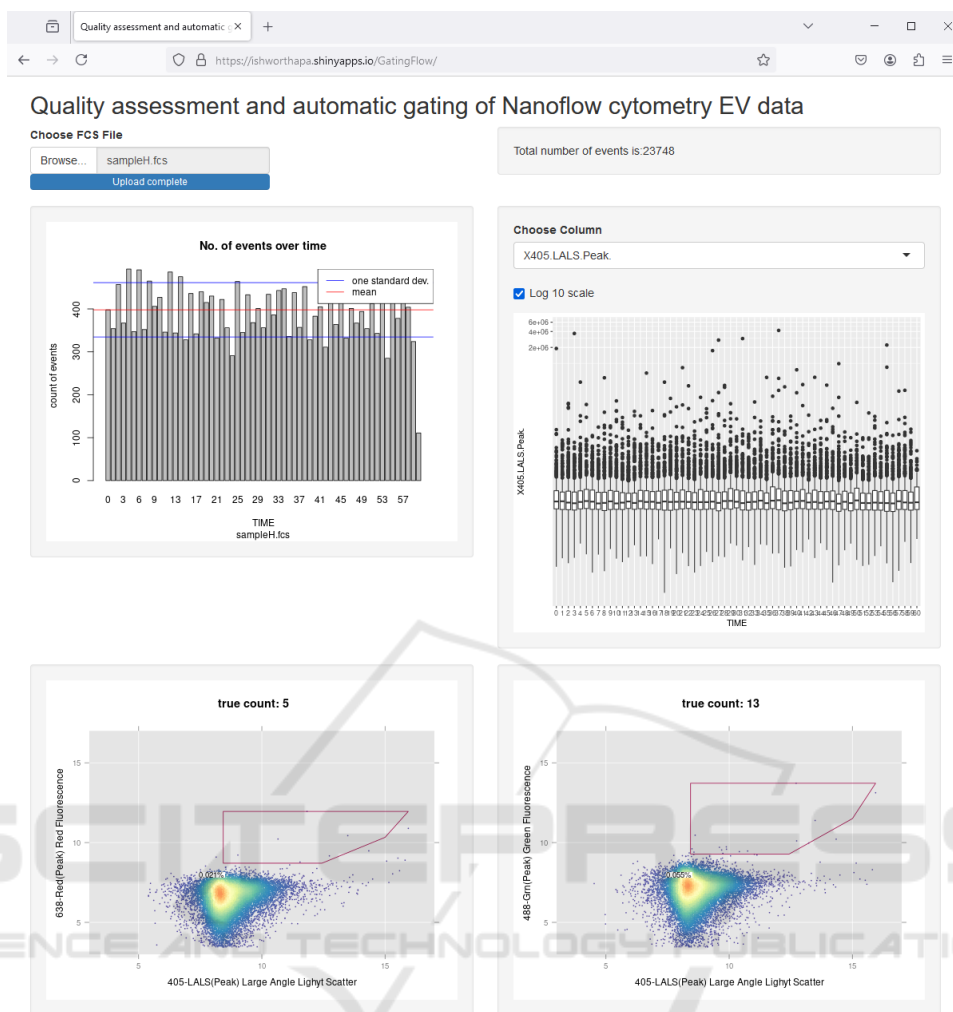


Figure 5: A snapshot of the Shiny web application.

Mathematical formulation of five-sided gating is listed in an algorithm (see **Algorithm 2**). A R program is written to implement this refined gating algorithm in order to count the positive events within these gates. The *filter()* function from *flowCore* R package is utilized for enumerating the sub-population of events in the gate (Hahne et al., 2009). Additionally, the *flowViz* R package that is compatible with data structures defined in the *flowCore* package is utilized for plotting the figures with the gates (Sarkar et al., 2008).

### 2.5 Shiny R App for Automated Gating

An open-source R package called, *Shiny* is utilized to create a web application for the quality assessment and automated gating. The automated gating in this app utilizes the five-sided gating strategy de-

scribed in **Algorithm 2**. The Shiny app is available at the following URL: <https://ishworthapa.shinyapps.io/gatingflow/>. In this web application, users can upload a FCS file for which the quality check and the automated gating procedure will be carried out. A snapshot of the user-interface is shown in Figure 5.

## 3 RESULTS

Next, we apply the quality checking step and automated gating algorithm on a real dataset from patient samples using the Shiny app. The quality check feature provides a quick and effective way to identify samples that are erroneous. Additionally, automated gating algorithm performs sample specific gating that accurately identifies the sub-population of events.



### 3.1 Quality Check Identifies Run with Erroneous Data

By plotting the values from different channels and *TIME* variable, the web application provided easy mechanism to identify samples with errors. For an instance, samples that saved time information incorrectly were easily captured (see Figure 6). In this sample, the timeline represented by X-axis is incorrect and should span from 0 to 60. In sample(s) that passed the quality checking step, like the one shown in Figure 2, the plots provided assurance that the acquisition process remained consistent and did not show any signs of deterioration over the observed time period.

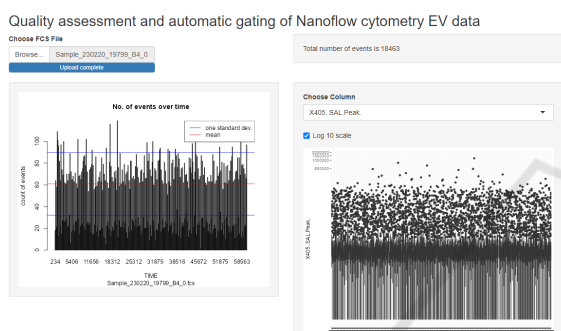


Figure 6: An example sample with erroneous data in the ‘TIME’ column of the FCS file.

### 3.2 Automated Gating

Antibody labeling was performed with two markers in the urine samples of cancer patients. A total of 90 FCS files (30 samples with 3 replicates each) were analyzed using the automated gating algorithm within the Shiny application. Between different marker proteins, the five-sided automated gating shows appropriate selection of boundary between the noise and the signal (see Figure 7). Additionally, to standardize the counts from different experiments, the number of positive events identified in automated gating was translated into a scaled number with appropriate dilution factor obtained from wet-lab protocol.

### 3.3 Comparison of Automated and Manual Gating Results

The final enumeration of positive EVs were then compared between both automated gating strategies (rectangular and five-sided) and manual gating performed by two independent reviewers. The comparison of the standardized number of events (in log10 scale) from both methods are shown in Figure 8. For *PSMA*



Figure 7: Automated (five-sided) gating results for two different markers showing accurate predictions of the gating boundaries.

marker positive EVs, the counts from automated gating are slightly less than those obtained from manual gating process. For *STEAP1* marker positive EVs, the counts from the automated and manual gating results fluctuate between samples as shown in Figure 8. For both markers, the five-sided automated gating resulted in less positive events than the rectangular gating by avoiding the points on the far right side of the rectangular gating. Overall, the results show that the automated gating is comparable to the manual gating, especially for *PSMA* marker positive EVs.

Next, we investigated the correlation between the gating results. As shown in Table 1, the Spearman’s rank correlation value between manual gating from two independent reviewers was 0.90 and 0.59 for *PSMA* and *STEAP1* markers, respectively. Interestingly, correlation between manual gating from second user and the automated gating approaches for *PSMA* marker was the highest ( $\rho = 0.87$ ). The correlation values for *STEAP1* marker are less than that for *PSMA* marker.

In addition, intraclass correlation coefficient

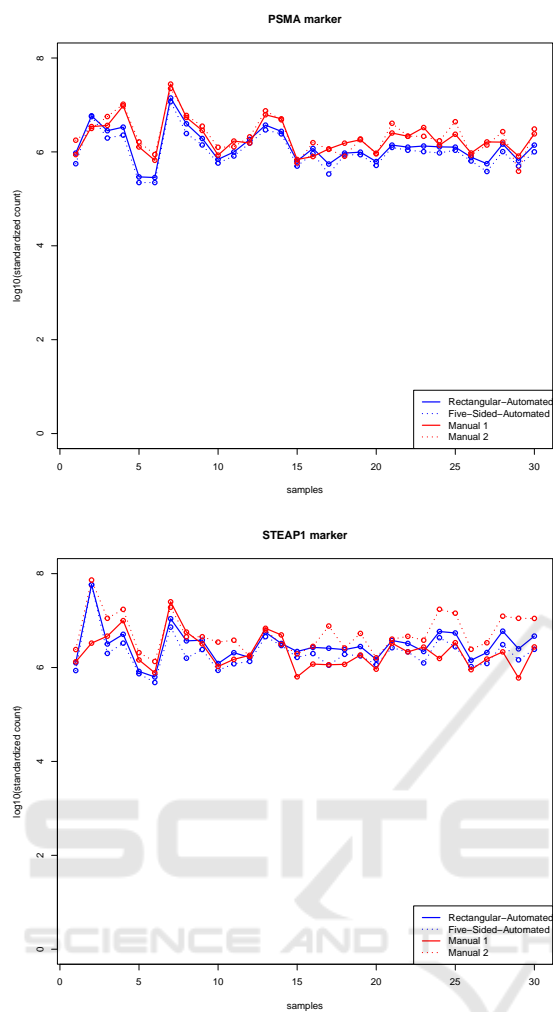


Figure 8: Manual versus automated gating results for *PSMA* and *STEAP1* markers (in log10 scale).

(ICC) was computed to measure index of inter-rater reliability of quantitative data using ‘*irr*’ R package. When comparing automated gating results with the manual gating results from first reviewer, the intra-class correlation value for *PSMA* and *STEAP1* markers were observed to be 0.73 and 0.51, respectively. Similarly, when comparing automated gating results with the manual gating results from second reviewer, ICC for *PSMA* and *STEAP1* markers were 0.751 and 0.9, respectively. Together, these results show that the automated gating enumeration is comparable to that of manual gating performed by experienced personnel.

Table 1: Spearman’s rank correlation between gating results for each marker ( $P - value < 0.01$ ).

Correlation groups	comparison	<i>PSMA</i>	<i>STEAP1</i>
Manual	Reviewer1-vs-Manual Reviewer2	0.90	0.59
Automated: Rectangular-vs-Manual	Reviewer1	0.85	0.74
Automated: Rectangular-vs-Manual	Reviewer2	0.87	0.85
Automated: Five-sided-vs-Manual	Reviewer1	0.86	0.73
Automated: Five-sided-vs-Manual	Reviewer2	0.87	0.73

## 4 CONCLUSIONS

This study proposed a novel computational platform for processing of high-resolution Flow Cytometry (hrFC) data from EV studies. We provide an automated method for checking the quality of cytometry data and algorithms to perform quantification of positive events in hrFC. In addition, we developed a web application that performs the quality checking step and automatically identifies the gate for sub-population of EVs that were otherwise enumerated by creating the boundaries manually. We showed that the manual gating step can vary between the individuals who perform the gating and is time consuming and not reproducible. However, our proposed algorithm is robust, deterministic, and always produces consistent gating highlighting the reproducible feature of our method. Currently, our web application is at the prototype stage to highlight the relevance of our pipeline and is compatible with data generated by Apogee A60-Micro Plus flow cytometer. Additional validation studies with larger number of samples are required to ensure the reliability and accuracy of our results, involving a larger pool of human reviewers for manual gating. In the future, we plan to enhance the app to allow multiple FCS files and accommodate other instruments. A study like ours is critical to facilitate EV-based biomarker studies for the development of innovative, next-generation molecular diagnostics in cancer. Accurate quantification and characterization of EVs in modern oncology will play a pivotal role in identifying prognostic, diagnostic and predictive markers in everyday medical practice. Before reaching the clinic, limitations such as imprecise EV clustering and traditional manual gating need to be replaced.

## ACKNOWLEDGEMENTS

The authors would like to acknowledge Daniel Quest, PhD from Mayo Clinic in constructive feedback during our meetings.

## REFERENCES

- Aharon, A., Spector, P., Ahmad, R. S., Horrany, N., Sabbach, A., Brenner, B., and Aharon-Peretz, J. (2020). Extracellular vesicles of alzheimer's disease patients as a biomarker for disease progression. *Molecular neurobiology*, 57:4156–4169.
- Arce, J. E., Welsh, J. A., Cook, S., Tigges, J., Ghiran, I., Jones, J. C., Jackson, A., Roth, M., and Milosavljevic, A. (2023). The nanoflow repository. *Bioinformatics*, 39(6):btad368.
- Ellison, T. J., Stice, S. L., and Yao, Y. (2023). Therapeutic and diagnostic potential of extracellular vesicles in amyotrophic lateral sclerosis. *Extracellular Vesicle*, 2:100019.
- Hahne, F., LeMeur, N., Brinkman, R. R., Ellis, B., Haaland, P., Sarkar, D., Spidlen, J., Strain, E., and Gentleman, R. (2009). flowcore: a bioconductor package for high throughput flow cytometry. *BMC bioinformatics*, 10(1):1–8.
- Kim, Y., Van Der Pol, E., Arafa, A., Thapa, I., Britton, C. J., Kostic, J., Song, S., Joshi, V. B., Erickson, R. M., Ali, H., et al. (2022). Calibration and standardization of extracellular vesicle measurements by flow cytometry for translational prostate cancer research. *Nanoscale*, 14(27):9781–9795.
- Lucien, F., Kim, Y., Qian, J., Orme, J. J., Zhang, H., Arafa, A., Abrahama, F., Thapa, I., Tryggestad, E. J., Harmesen, W. S., et al. (2022). Tumor-derived extracellular vesicles predict clinical outcomes in oligometastatic prostate cancer and suppress antitumor immunity. *International Journal of Radiation Oncology\* Biology\* Physics*, 114(4):725–737.
- Newman, L. A., Muller, K., and Rowland, A. (2022). Circulating cell-specific extracellular vesicles as biomarkers for the diagnosis and monitoring of chronic liver diseases. *Cellular and Molecular Life Sciences*, 79(5):232.
- Ohmichi, T., Mitsuhashi, M., Tatebe, H., Kasai, T., El-Agnaf, O. M. A., and Tokuda, T. (2019). Quantification of brain-derived extracellular vesicles in plasma as a biomarker to diagnose parkinson's and related diseases. *Parkinsonism & related disorders*, 61:82–87.
- Pan, Y., Lu, X., Shu, G., Cen, J., Lu, J., Zhou, M., Huang, K., Dong, J., Li, J., Lin, H., et al. (2023). Extracellular vesicle-mediated transfer of lncrna igfl2-as1 confers sunitinib resistance in renal cell carcinoma. *Cancer Research*, 83(1):103–116.
- Salmond, N., Khanna, K., Owen, G. R., and Williams, K. C. (2021). Nanoscale flow cytometry for immunophenotyping and quantitating extracellular vesicles in blood plasma. *Nanoscale*, 13(3):2012–2025.
- Samuel, P., Mulcahy, L. A., Furlong, F., McCarthy, H. O., Brooks, S. A., Fabbri, M., Pink, R. C., and Carter, D. R. F. (2018). Cisplatin induces the release of extracellular vesicles from ovarian cancer cells that can induce invasiveness and drug resistance in bystander cells. *Philosophical Transactions of the Royal Society B: Biological Sciences*, 373(1737):20170065.
- Sarkar, D., Le Meur, N., and Gentleman, R. (2008). Using flowviz to visualize flow cytometry data. *Bioinformatics*, 24(6):878–879.
- Spidlen, J., Moore, W., Parks, D., Goldberg, M., Blenman, K., Cavanaugh, J. S., Force, I. D. S. T., and Brinkman, R. (2021). Data file standard for flow cytometry, version fcs 3.2. *Cytometry Part A*, 99(1):100–102.
- Spidlen, J., Moore, W., Parks, D., Goldberg, M., Bray, C., Bierre, P., Gorombey, P., Hyun, B., Hubbard, M., Lange, S., et al. (2010). Data file standard for flow cytometry, version fcs 3.1. *Cytometry Part A: The Journal of the International Society for Advancement of Cytometry*, 77(1):97–100.
- Théry, C., Witwer, K. W., Aikawa, E., Alcaraz, M. J., Anderson, J. D., Andriantsitohaina, R., Antoniou, A., Arab, T., Archer, F., Atkin-Smith, G. K., et al. (2018). Minimal information for studies of extracellular vesicles 2018 (misev2018): a position statement of the international society for extracellular vesicles and update of the misev2014 guidelines. *Journal of extracellular vesicles*, 7(1):1535750.
- van der Pol, E., Sturk, A., van Leeuwen, T., Nieuwland, R., Coumans, F., Mobarrez, F., Arkesteijn, G., Wauben, M., Siljander, P.-M., Sánchez-López, V., et al. (2018). Standardization of extracellular vesicle measurements by flow cytometry through vesicle diameter approximation. *Journal of thrombosis and haemostasis*, 16(6):1236–1245.
- Welsh, J. A., Horak, P., Wilkinson, J. S., Ford, V. J., Jones, J. C., Smith, D., Holloway, J. A., and Englyst, N. A. (2020a). Fcypass software aids extracellular vesicle light scatter standardization. *Cytometry Part A*, 97(6):569–581.
- Welsh, J. A., Van Der Pol, E., Arkesteijn, G. J., Bremer, M., Brisson, A., Coumans, F., Dignat-George, F., Duggan, E., Ghiran, I., Giebel, B., et al. (2020b). Miflowcyte: A framework for standardized reporting of extracellular vesicle flow cytometry experiments. *Journal of extracellular vesicles*, 9(1):1713526.